IEEE Access
Multidisciplinary | Rapid Review | Open Access Journal

Received March 14, 2020, accepted March 25, 2020, date of publication April 1, 2020, date of current version April 15, 2020.

*Digital Object Identifier 10.1109/ACCESS.2020.2984934*

# Effects of Textile Weaving and Finishing Processes on Textile-Based Wearable Patch Antennas

**RIA APRILLIYANI[1], PHILIP AYIKU DZAGBLETEY[2], (Member, IEEE), JUNG HUN LEE[3], MYOUNG JIN JANG[4], JU-HEE SO[3], AND JAE-YOUNG CHUNG[2], (Senior Member, IEEE)**

[1]Integrated IT Engineering Department, Seoul National University of Science and Technology, Seoul 01811, South Korea
[2]Electrical and Information Department, Seoul National University of Science and Technology, Seoul 01811, South Korea
[3]Human Convergence Technology R&D Group, Korea Institute of Industrial Technology (KITECH), Ansan 31056, South Korea
[4]Korea Textile Development Institute (KTDI), Daegu 41842, South Korea

Corresponding authors: Ju-Hee So (jso@kitech.re.kr) and Jae-Young Chung (jychung@seoultech.ac.kr)

This work was supported in part by the Ministry of Trade, Industry and Energy (MOTIE) and Korea Institute for Advancement of Technology (KIAT) through the Academia-Industry International Collaboration Program, under Grant P0005438, and in part by the Basic Science Research Program through the National Research Foundation of Korea (NRF) funded by the Ministry of Education under Grant NRF-2019R1A6A1A03032119.

**ABSTRACT** In this paper, we analyze the effects of textile weaving and finishing processes on the performance of textile-based wearable antennas. Several textile-based patch antennas operating at 2.4 GHz were designed and fabricated for evaluation. All of them had the same geometry comprising a 1-mm-thick felt substrate in the middle, and silver ink screen-printed polyester fabric as the ground and patch at the bottom and on top. However, polyester fabric, the bare textile material for the conductive ground and patch was subjected to different weaving and finishing (tentering, scouring, and calendering) processes. It was observed that the antenna resonant frequency, bandwidth, radiation efficiency, and peak gain were varied by these processes, although the antenna geometry and screen-printing method were identical to each other. The best antenna exhibits a peak gain of 5.2 dBi and a radiation efficiency of 42.4%, while the worst shows corresponding values of 4.17 dBi and 34.8%. This implies that the weaving and finishing processes considerably impact textile-based wearable antenna performances.

**INDEX TERMS** Conductive ink, conductive textile, patch antenna, screen printing, textile-based antenna, wearable antenna, weaving process.

## I. INTRODUCTION

Wearable electronics have been gaining increasing attention with maturity of the Internet-of-Things (IoT) business. According to a market forecast [1], the total revenue for wearables is set to increase from approximately $50 billion in 2019 to $150 billion in 2023. Currently, most of the wearable electronics are in the form of separate gadgets such as watches, headphones, eyewear, and helmets. In the near future, however, many anticipate ''Truly wearable devices'' such as implants or tattoo to dominate the market [2], [3].

Meanwhile, ''smart clothing'' [4] is a promising wearable application that is intuitively better than a gadget and less invasive than a body-implanted device. The success of smart clothing strongly depends on textile technology because electronic components on clothes must be conformal and flexible. Therefore, ''smart textile'' is being actively developed for wearable electronics. The value of the global smart textile market is reported to reach more than $9,000 million in 2024 with an exponential increase thereafter [5].

Smart clothing is applicable in the medical, sports, military, and fashion areas. Regardless of the application, a radio frequency (RF) wireless communication function is essential for sharing information with an external device. The production of such high frequency (∼GHz) electronic components for wireless communication is more challenging than manufacturing DC or low frequency (∼kHz) components (e.g., actuators or sensors). This is because the low conductivity of textiles usually ranges from $10^4$–$10^6$ S/m [6], [7] compared with metals (e.g., $10^7$ S/m for copper), thereby resulting in a

The associate editor coordinating the review of this manuscript and approving it for publication was Yingsong Li.

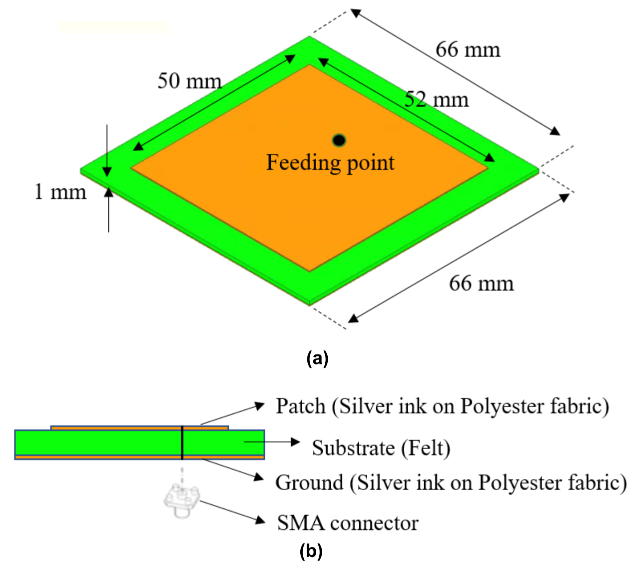


**FIGURE 1. The antenna geometry applied for all the tested antennas: (a) Top view and (b) Side view.**

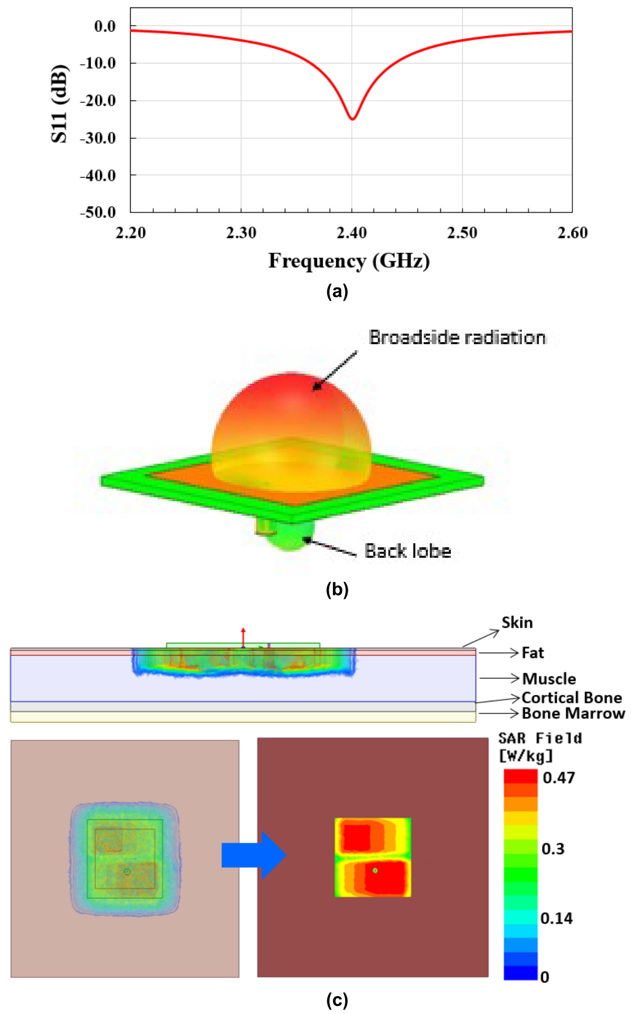


**FIGURE 2. Simulation results of (a) S11 response, (b) 3D radiation pattern, and (c) Specific absorption rate.**

higher power loss as high frequency currents flow through a conductive textile. This property considerably limits the radiation efficiency of a wearable antenna [8]–[11].

Taking cognizance of the low conductivity limitation is inevitable for a textile-based wearable antenna, we investigated the effects of textile properties on the antenna performance in this paper. Specifically, we varied the weaving and finishing processes (i.e., tentering, scouring, and calendering) of bare textile (i.e., polyester textile), and then compared the radiation efficiency, peak gain, and resonant frequency of the wearable antennas. Excluding the weaving and finishing processes, all the tested antennas had an identical feature: a bottom-fed patch antenna with a 1-mm-thick felt substrate in the middle. The bottom and top conductive layers (i.e., ground and patch, respectively) were produced via screen-printing the same conductive ink on the polyester textile. Thus, we could specifically examine the effects of textile properties on the antenna performance. Several studies have reported how antenna geometry or conductive ink property affects the performance of wearable antennas [8]–[11]. However, to the best of our knowledge, this is the first study reporting the impact of textile weaving and finishing processes on textile-based wearable antenna performance.

## II. PATCH ANTENNA DESIGN AND SIMULATION

A simple patch antenna resonating at 2.4 GHz was designed using a full-wave 3D electromagnetic simulator, ANSYS® HFSS™. Simulation results, including the antenna reflection coefficient, gain, efficiency, radiation pattern, and specific absorption rate (SAR), were obtained by assigning material properties of the felt substrate and conductive ink used in the actual design. Based on these results, antennas were fabricated and tested, as explained in Sections III and IV.

### A. ANTENNA CONFIGURATION

Figures 1(a) and (b) display the top and side views of the patch antenna model, with the antenna comprising a top patch, middle substrate, and bottom ground. The patch and ground were polyester fabrics that were screen-printed with conductive ink. The thickness of the conductive ground and patch was 0.12 mm for each sheet. The conductive ink was Electrodag 479SS silver ink from Henkel Achenson with a sheet resistivity of 0.02 Ω/sq/mil [12]. The bulk resistivity and conductivity deduced from the sheet resistivity were $5.08 \times 10^{-7}\ \Omega m$ and $1.97 \times 10^{6}\ S/m$, respectively. This bulk conductivity ($\sigma$) was assigned in HFSS for the ground and patch. Additionally, the dielectric constant($\varepsilon_r$) and the loss tangent (tan$\delta$) of the felt substrate assigned were 1.36 and 0.02, respectively [13].

### B. ANTENNA SIMULATION RESULT

In HFSS, the patch antenna was optimized to resonate at 2.4 GHz. The optimized length and width parameters are displayed in Fig. 1(a), and the simulation results are exhibited in Fig. 2. As observed from the graph of simulated reflection coefficient (S11) in Fig. 2(a), the antenna successfully resonates at 2.4 GHz with a bandwidth of 80 MHz (2.36–2.44 GHz).

The 3D radiation pattern of the antenna in Fig. 2(b) reflects a traditional broadside radiating pattern with a low back lobe. The patch antenna is the preferred design for wearable applications because of its simple structure and low back radiation toward the human body associated with its ground.

Figure 2(c) shows the SAR simulation result estimated by placing the antenna on a 5-layer human body mimicking phantom. The thicknesses and material properties of each layer were properly assigned based on [14]: skin (0.9 mm), fat (2.2 mm), muscle (19.7 mm), cortical bone (4.3 mm), and bone marrow (4.66 mm), in a top-down order.

The input power to the antenna was set to 0.1 W, which was usual for most 2.4-GHz low power devices. The calculated SAR field in Fig. 2(c) shows that most absorption occurs in the top three layers (skin, fat and muscle), and the average SAR value of 0.47 W/kg (10 g) is below the certified value (i.e., 2 W/kg) [15].

## III. TEXTILE PROCESS AND ANTENNA FABRICATION

After obtaining the optimized geometry for the wearable patch antenna, we fabricated antennas with the same geometry but different bare textiles (i.e., polyester fabric). The differences originated from the weaving, tentering, scouring, and calendering processes applied on the bare textile. The processed textiles were screen-printed with silver ink and then used for fabricating the antennas. Before describing the antenna fabrication, we have explained each textile weaving and finishing processes in the part that follows.

### A. WEAVING PROCESS

The polyester fabric was created by weaving a bundle of polyester yarns. That is, each warp (vertical) and weft (horizontal) yarn alternately cross under and over each other in a certain pattern. Many weaving patterns such as plain, matt (or basket weave), twill, satin, jacquard, and pile exist. In here, we examined plain and matt that are considered to be the simplest and most widely used weaving patterns. Figure 3(a) and (b) illustrates the woven structure of plain and matt. The hardness of plain weave is 2H (i.e. crossing of a single warp and weft yarn), while that of matt weave is 4H (i.e. crossing of two warp and weft yarns). This results in a higher density of matt weave (140 × 140) than the plain weave (108 × 106). Some literatures pointed out the effects of weaving pattern on the performance of ink-jet printed [16], [17] and embroidered electronics [18], [19]. We also expected that the weaving pattern would affect the antenna performance because the amount of silver ink absorption might vary on account of it. Note that that the yarn used to weave was polyester flat yarns [20] that offered higher density woven fabric compared with conventional round yarns.

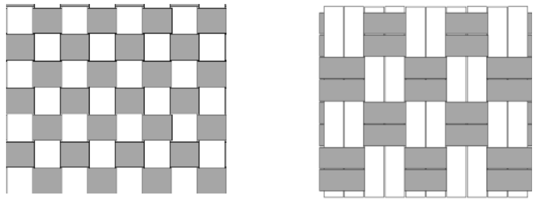

(a) (b)

**FIGURE 3.** Weaving patterns: (a) Plain and (b) Matt weave.

(a) (b)

**FIGURE 4.** Machines used for textile finishing processes: (a) Tenter and (b) Drum machine for tentering and scouring, respectively (Courtesy of Korea Textile Development Institute).

### B. TENTERING AND SCOURING PROCESS

Tentering and scouring are the most important textile finishing processes. The purpose of tentering is straightening the textile and removing leftover water. This occurs in a tenter by blasting the textile with hot air while rolling on cylinders. Conversely, the scouring process eliminates impurities (oil, gums, and dirt), thereby assisting the textile to remain highly absorptive during the printing process [21]. The tenter and drum machine used for the tentering and scouring processes in this study are shown in Fig. 4. We compared the performance of antennas fabricated using textiles with and without these processes, i.e., tentering, scouring, and heating (170°C).

### C. CALENDERING PROCESS

Calendering is the last textile finishing process applied on the bare textile. It comprises passing the textile between rollers under appropriate heat and pressure. The process improves the flatness and smoothness of the textile before printing. The roller machine used in this study is displayed in Fig. 5, while the textile cross-sections obtained from scanning electron microscopy (SEM) are exhibited in Fig.6. Clearly, the calendering process effectively flattens and smoothens the textile surface.

### D. PATCH ANTENNA FABRICATION

The fabricated patch antennas were identical in geometry, but their bare textiles were subjected to diverse weaving and finishing processes. The conductive ink was printed on the processed textiles using the SP5080EP automatic screen printer from the Korea Institute of Industrial Technology. The textiles with printed conductive ink were then accurately trimmed to the desired dimensions using the Cricut®

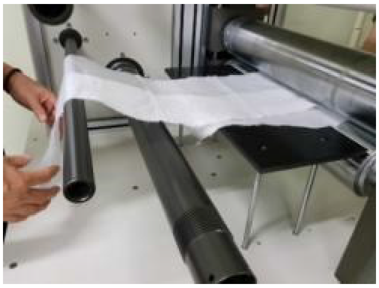

**FIGURE 5.** The roller machine used for the calendering process. (Courtesy of Korea Textile Development Institute).

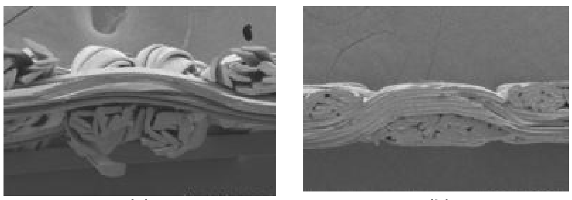

(a) (b)

**FIGURE 6.** Cross-sections of the polyester textiles obtained by SEM: (a) before calendering and (b) after calendering. (Courtesy of Korea Institute of Industrial Technology).

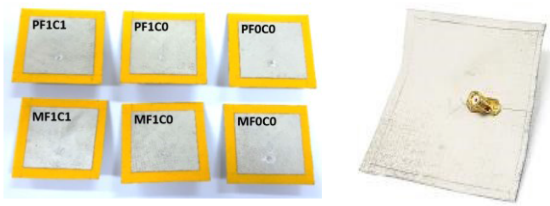


(a) (b)

**FIGURE 7.** Fabricated wearable patch antennas including: (a) antenna samples fabricated from different bare textile processes, and (b) the rear side of the antenna.

cutting machine. These textiles were placed above and below the felt substrate and fed by an SMA coaxial connector. The latter was attached to the ground layer using conductive epoxy, Chemtronics CW2400. Figure 7(a) shows the fabricated patch antennas. A closer view of the rear side of the antenna including the SMA connector can be observed in Fig. 7(b). The labels in Fig. 7(a) indicate the weaving and finishing processes used for the textiles. For example, PF1C1 implies the antenna fabricated using the textile with plane weave, gone through the finishing processes, and gone through the calendaring process. MF1C0 implies the textile with matt weave, gone through finishing processes, but no calendaring applied.

## IV. MEASUREMENT RESULTS AND COMPARISON

In this section, the antenna measurement results are compared to understand the effects of the weaving, tentering, scouring, and calendering processes on the textile-based antenna performance. The reflection coefficients of the fabricated antennas were measured using a network analyzer, while the radiation patterns were measured in an anechoic chamber.

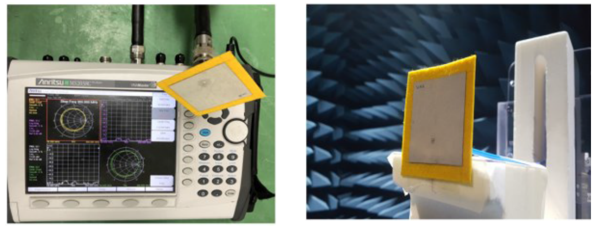

(a) (b)

**FIGURE 8.** Antenna measurements for: (a) the reflection coefficient using a network analyzer, and (b) the radiation pattern in an anechoic chamber.

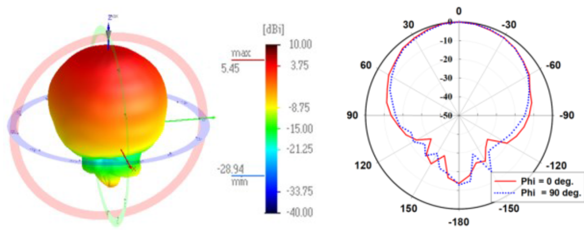


(a) (b)

**FIGURE 9.** Examples of the measured radiation patterns in (a) 3D and (b) 2D graph.

Figures 8(a) and (b) show the antenna connected with the network analyzer (Anritsu MS2038C) and mounted in the anechoic chamber (Electromagnetic Wave Technology Institute in Seoul), respectively. The measured 3D and 2D radiation patterns for one of the wearable patch antennas are exhibited in Fig. 9. A broadside radiation pattern resembling the simulation result in Fig. 2(b) is evident. All the tested antennas display similar broadside radiation patterns, but have different peak gain and radiation efficiency values. These differences have been discussed in the following subsections.

### A. EFFECT OF THE WEAVING PROCESS

A comparison of the measured S11 for antennas fabricated with plain and matt woven textiles is displayed in Fig. 10. The plain weave antenna exhibits a higher resonant frequency (2.36 GHz) than that with the matt weave (2.31 GHz). Additionally, the resonance of the plain weave antenna is sharper with a narrower S11 $< -10$ dB bandwidth (50 MHz) than that of the matt weave antenna (70 MHz). These details have been listed in Table 1 together with the quality factor ($Q$) of the antennas. $Q$ is defined as the ratio of the energy stored and dissipated in a cycle of oscillation and is represented by

$$Q = 2\pi \frac{\text{Energy stored}}{\text{Energy dissapated per cycle}}. \qquad (1)$$

Considering an antenna as an RLC tank circuit, $Q$ is calculated as the ratio of the resistive ($R$) and reactive ($X$) components at the resonant frequency ($f_r$) [22]. This is further approximated as the inverse of the fractional bandwidth and

**TABLE 1.** Comparison of plain and matt weave.

| | Bandwidth (GHz) | Resonant frequency (GHz) | Quality factor | Peak Gain (dBi) | Rad. Eff. (%) |
|---|---|---|---|---|---|
| Plain Weave | 2.34–2.39 (50 MHz) | 2.36 | 47.2 | 5.2 | 42.44 |
| Matt Weave | 2.27–2.34 (70 MHz) | 2.31 | 33 | 4.98 | 41.9 |

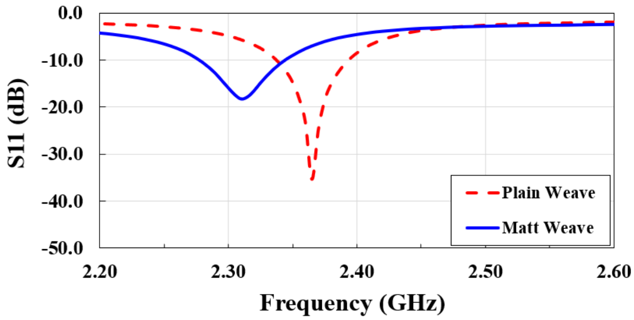


**FIGURE 10.** Comparison of the S11 for the plain and matt woven antennas showing a shaper narrower resonant frequency for the plain weave antenna.

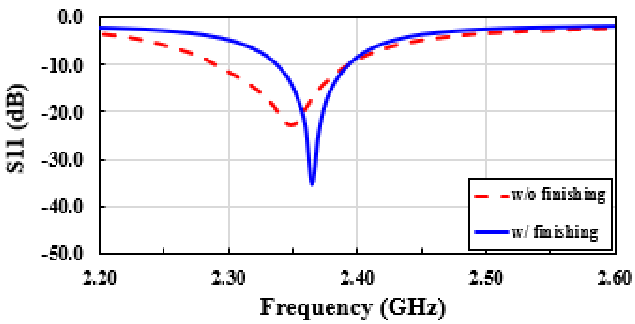


**FIGURE 11.** Comparison of S11 with and without finishing processes (tentering and scouring).

represented as

$$Q \approx \frac{2\pi f_r}{2R\,(f_r)}\,|X\,(f_r)| \approx \frac{f_r}{f_u - f_l}, \qquad (2)$$

where $f_u$ and $f_l$ are the upper and lower frequency of the bandwidth. Here, the S11 $<$ $-10$ dB criterion is used.

Based on the measured $f_r$, $f_u$, and $f_l$, the $Q$ values obtained of the plain and matt woven antennas are 47.2 and 33, respectively. A higher $Q$ value indicates sharper resonance, narrower bandwidth, less power dissipated, and higher radiation efficiency. As observed in Table 1, both the measured radiation efficiency and peak gain for the higher $Q$ plain weave case are higher than those of the lower $Q$ matt weave case. Less dissipation occurs in the plain weave possibly because of its denser woven structure, thereby allowing the conductive ink to be absorbed in the textile with more conformity.

**TABLE 2.** Comparison of w/ and w/o finishing process.

| | Bandwidth (GHz) | Resonant frequency (GHz) | Quality factor | Peak Gain (dBi) | Rad. Eff. (%) |
|---|---|---|---|---|---|
| w/o finishing | 2.29–2.39 (100 MHz) | 2.35 | 23.5 | 4.17 | 34.76 |
| w/ finishing | 2.34–2.39 (50 MHz) | 2.36 | 47.2 | 5.2 | 42.44 |

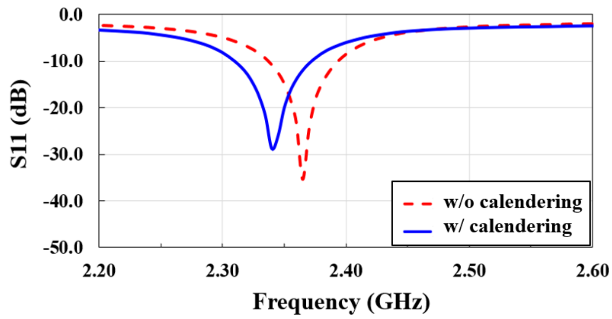


**FIGURE 12.** Comparison of S11 with and without calendering processes.

**TABLE 3.** Comparison of w/ and w/o calendering process.

| | Bandwidth (GHz) | Resonant frequency (GHz) | Quality factor | Peak Gain (dBi) | Rad. Eff. (%) |
|---|---|---|---|---|---|
| w/o calendering | 2.34–2.39 (50 MHz) | 2.36 | 47.2 | 5.2 | 42.44 |
| w/ calendering | 2.31–2.37 (60 MHz) | 2.34 | 39 | 4.83 | 39.18 |

### B. EFFECT OF THE TENTERING AND SCOURING PROCESSES

The S11 responses of antennas fabricated using plain weave polyester textiles with and without finishing processes (tentering and scouring) are shown in Fig. 11. Evidently, the finishing processes reduce the bandwidth (from 100 to 50 MHz) and increase the resonant frequency (from 2.35 to 2.36 GHz), implying a higher $Q$ with lower dissipation. This is reflected in the higher radiation efficiency and peak gain for this textile as shown in Table 2. This infers that removing water and gums in textile by the tentering and scouring processes is highly recommended. They are known to reduce the surface roughness of the textile, thus improving the printability of the conductive ink and resulting in a higher effective conductivity of the printed textile [21].

### C. EFFECT OF THE CALENDERING PROCESS

The S11 responses of antennas with textiles with and without the calendering process are compared in Fig. 12. These antennas involve plain weaving, tentering, and scouring. The data in Table 3 reveals that calendering is unnecessary because it lowers $Q$, peak gain, and radiation efficiency. This is unexpected considering that in Fig. 6, the SEM images show a smoother textile cross-section after calendering. Possibly, the coarser surface is beneficial for smearing the ink into the textile, thereby causing lower dissipation as the high frequency currents travel.

## V. CONCLUSION

We conducted a study to evaluate the impact of textile weaving and finishing processes (tentering, scouring, and calendering) on the performance of textile-based wearable antennas. A broadside radiating patch antenna preferable for wearable applications was implemented via a full-wave electromagnetic simulation tool, and its S11, radiation pattern, gain, and SAR were calculated and verified. Based on this design, several antennas were fabricated, and their parameters were measured and compared.

The measured results showed that peak gain and radiation efficiency of the plain weave antenna were higher than those of the matt woven antenna. Moreover, the tentering and scouring processes increased $Q$ of the antenna, thereby resulting in a higher gain and radiation efficiency; however, the calendering process did not prove to be suitable. It was not only an expensive and time consuming process to flatten the textile but also decreased the gain and efficiency of the textile based antenna. Such relationships between the textile processes and antenna parameters were consistently observed in other antenna sample testing results.

The fact that $Q$ of an antenna is related to the effective conductivity of the material used is well known. This study shows that the effective conductivity of a conductive textile can be varied not only via conductive ink properties or printing processes, but also via bare textile weaving and finishing processes. Our ongoing multidisciplinary research with electrical and textile engineering experts focuses on quantifying effective conductivity caused by textile property changes.

## REFERENCES

[1] IDTechEx Research. *Wearables Market Outlook 2020: Drivers and New Markets*. Accessed: Sep. 17, 2019. [Online]. Available: https://www.i-scoop.eu/wearables-market-outlook-2020-drivers-new-markets/

[2] Allied Market Research. *Implantable Medical Devices Market by Product (Orthopedic Implants, Dental Implants, Breast Implants, Cardiovascular Implants, Intraocular Lens, and Other Implants)—Global Opportunity Analysis and Industry Forecast, 2014–2022*. Accessed: Jan. 2, 2020. [Online]. Available: https://www.alliedmarketresearch.com/implantable-medical-devices-market

[3] Market Study Report. *Global Smart Tattoo Market Growth (Status and Outlook) 2019–2024*. Accessed: Jan. 2, 2020. [Online]. Available: https://www.marketstudyreport.com/reports/global-smart-tattoo-market-growth-status-and-outlook-2019-2024

[4] F. Axisa, P. M. Schmitt, C. Gehin, G. Delhomme, E. McAdams, and A. Dittmar, "Flexible technologies and smart clothing for citizen medicine, home healthcare, and disease prevention," *IEEE Trans. Inf. Technol. Biomed.*, vol. 9, no. 3, pp. 325–336, Sep. 2005, doi: 10.1109/TITB.2005.854505.

[5] Ameri Research. *Smart Textiles Market to 2024*. Accessed: Sep. 17, 2019. [Online]. Available: https://www.ameriresearch.com/product/smart-textiles-market/

[6] J.-Y. Chung, N. K. Nahar, L. Zhang, Y. Bayram, K. Sertel, and J. L. Volakis, "Broadband RF conductivity measurement technique for engineered composites," *IET Microw., Antennas Propag.*, vol. 6, no. 4, pp. 371–376, 2012.

[7] E. Yilmaz, D. P. Kasilingam, and B. M. Notaros, "Performance analysis of wearable microstrip antennas with low-conductivity materials," in *Proc. IEEE Antennas Propag. Soc. Int. Symp.*, San Diego, CA, USA, Jul. 2008, pp. 1–4.

[8] K. N. Paracha, S. K. A. Rahim, P. J. Soh, and M. Khalily, "Wearable antennas: A review of materials, structures, and innovative features for autonomous communication and sensing," *IEEE Access*, vol. 7, pp. 56694–56712, 2019, doi: 10.1109/ACCESS.2019.2909146.

[9] C. Hertleer, H. Rogier, L. Vallozzi, and L. Van Langenhove, "A textile antenna for off-body communication integrated into protective clothing for firefighters," *IEEE Trans. Antennas Propag.*, vol. 57, no. 4, pp. 919–925, Apr. 2009, doi: 10.1109/TAP.2009.2014574.

[10] S. Lee and J. Choi, "All-textile corrugated ground SIW horn antenna for millimeter-wave WBAN applications," *J. Electromagn. Eng. Sci.*, vol. 19, no. 4, pp. 221–226, Oct. 2019.

[11] Y. Bayram, Y. Zhou, B. S. Shim, S. Xu, J. Zhu, N. A. Kotov, and J. L. Volakis, "E-textile conductors and polymer composites for conformal lightweight antennas," *IEEE Trans. Antennas Propag.*, vol. 58, no. 8, pp. 2732–2736, Aug. 2010, doi: 10.1109/TAP.2010.2050439.

[12] *Henkel Adhesive Technologies*. Accessed: Jan. 1, 2020. [Online]. Available: https://www.henkel-adhesives.com/us/en/product/inks-_-coatings/loctite_edag_479ssec.html

[13] P. M. Nguyen and J.-Y. Chung, "Characterisation of antenna substrate properties using surrogate-based optimisation," *IET Microw., Antennas Propag.*, vol. 9, no. 9, pp. 867–871, Jun. 2015.

[14] C. Gabriel, "Compilation of the dielectric properties of body tissues at RF and microwave frequencies," Brooks AFB, Brooks AFB, TX, USA, Tech. Rep. AL/OE-TR-1996-0037, 1996.

[15] *IEEE Standard for Safety Levels With Respect to Human Exposure to Radio Frequency Electromagnetic Fields, 3 KHz to 300 GHz*, IEEE Standard C95.1-2005, Apr. 2005.

[16] W. G. Whittow, A. Chauraya, J. C. Vardaxoglou, Y. Li, R. Torah, K. Yang, S. Beeby, and J. Tudor, "Inkjet-printed microstrip patch antennas realized on textile for wearable applications," *IEEE Antennas Wireless Propag. Lett.*, vol. 13, pp. 71–74, 2014.

[17] H. Shahariar, I. Kim, H. Soewardiman, and J. S. Jur, "Inkjet printing of reactive silver ink on textiles," *ACS Appl. Mater. Interfaces*, vol. 11, no. 6, pp. 6208–6216, Feb. 2019.

[18] T. M. Nguyen, J.-Y. Chung, and B. Lee, "Radiation characteristics of woven patch antennas composed of conductive threads," *IEEE Trans. Antennas Propag.*, vol. 63, no. 6, pp. 2796–2801, Jun. 2015.

[19] L. Alonso-González, S. Ver-Hoeye, M. Fernández-García, C. Vázquez-Antuña, and F. L.-H. Andrés, "From threads to smart textile: Parametric characterization and electromagnetic analysis of woven structures," *IEEE Access*, vol. 7, pp. 1486–1501, 2019.

[20] J. Hong, C. Jung, S. Yoon, and S. Choi, "A study on pre-treatment and performance evaluation for printing RFID antenna with conductive paste," *J. Korea Soc. Dyers Finishers*, vol. 25, no. 4, pp. 287–291, 2014.

[21] E. Shim, "Coating and laminating processes and techniques for textiles," in *Smart Textile Coatings and Laminates*. Washington, DC, USA: Elsevier, 2010, ch. 2, pp. 10–41.

[22] A. D. Yaghjian and S. R. Best, "Impedance, bandwidth, and Q of antennas," *IEEE Trans. Antennas Propag.*, vol. 53, no. 4, pp. 1298–1324, Apr. 2005.

**RIA APRILLIYANI** received the B.Eng. degree in electrical engineering from Universitas Indonesia, Indonesia, in 2017. She is currently pursuing the M.S. degree in integrated IT engineering with the Seoul National University of Science and Technology, Seoul, South Korea. She is also a Research Assistant with the Electromagnetic Measurement and Application Laboratory, Seoul National University of Science and Technology. Her research interest includes antenna design for wearable antenna application.

**PHILIP AYIKU DZAGBLETEY** (Member, IEEE) received the B.Sc. degree in telecommunication engineering from KNUST, Ghana, in 2013, and the M.Sc. degree from Hanbat University, South Korea, in 2016. He is currently pursuing the Ph.D. degree in electrical and information engineering with Seoultech University, South Korea. Much of his research interests have been in microwave and millimeter-wave antenna and circuit design for industrial and commercial use. He has completed a number of projects including 5G antenna measurement systems, millimeter-wave antenna array systems, and wearable fabric antennas.

**JUNG HUN LEE** received the B.S. and M.S. degrees from Konkuk University, South Korea, in 2015 and 2017, respectively. He is currently pursuing the Ph.D. degree with the Department of Materials Science and Engineering, Seoul National University, South Korea. He has been a Researcher with the Department of Human Convergence Technology Group, Korea Institute of Industrial Technology, South Korea, since 2018. His research interests include wearable textile applications based on conductive fibers/inks (KITECH) and carbon materials-based wearable, electronic fiber, and healthcare monitoring (SNU).

**MYOUNG JIN JANG** received the B.S. degree from Kyoungpook University, South Korea, in 2012, and the M.S. degree from the Gwangju Institute of Science and Technology, South Korea, in 2014. He is currently a Senior Researcher with the Korea Textile Development Institute, South Korea.

**JU-HEE SO** received the B.S. and M.S. degrees in chemical engineering from Seoul National University, Seoul, South Korea, in 2004 and 2006, respectively, and the Ph.D. degree in chemical and biomolecular engineering from North Carolina State University, Raleigh, NC, USA, in 2012. She was a Postdoctoral Researcher with the Department of Chemistry and Chemical Biology, Harvard University, from 2012 to 2015. She is currently a Senior Researcher with the Human Convergence Technology R&D Group, Korea Institute of Industrial Technology. Her research interests include E-textiles, wearables, nano-and micro fabrication, soft matter electronics, surface chemistry, and rheology.

**JAE-YOUNG CHUNG** (Senior Member, IEEE) received the B.S. degree from Yonsei University, South Korea, in 2002, and the M.S. and Ph.D. degrees from The Ohio State University, USA, in 2007 and 2010, respectively, all in electrical engineering. From 2002 to 2004, he was with Motorola Korea as an RF Engineer. From 2010 to 2012, he worked at Samsung Electronics, South Korea, as an Antenna Engineer. He is currently an Associate Professor with the Department of Electrical and Information Engineering, Seoul National University of Science and Technology, South Korea. His research interests include electromagnetic measurement and antenna design.